

High-efficiency ultra-precision comparator for *d*-spacing mapping measurement of silicon

Junliang Yang,^{a,b} Tang Li,^{a,b} Ye Zhu,^{a,b} Xiaowei Zhang,^{a*} Atsushi Waseda^c and Hiroyuki Fujimoto^{c,d}

^aInstitute of High Energy Physics, Chinese Academy of Science, Yuquan Road 19B, Shijingshan District, Beijing 100049, People's Republic of China, ^bUniversity of Chinese Academy of Science, Yuquan Road 19A, Shijingshan District, Beijing 100049, People's Republic of China, ^cNational Metrology Institute of Japan, AIST, 1-1-1 Umezono, Tsukuba 305-8563, Japan, and ^dAnalytical and Measuring Instruments Division, Shimadzu Corporation, 1-3 Kanda Nishiki-cho, Chiyoda-ku, Tokyo 101-8448, Japan. *Correspondence e-mail: zhangxw@ihep.ac.cn

Received 29 September 2019

Accepted 3 February 2020

Edited by Y. Amemiya, University of Tokyo, Japan

Keywords: self-referenced lattice comparator; *d*-spacing of silicon; 1D X-ray photon-counting detector; pencil beam; brush beam.

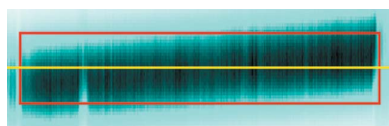
This article describes a high-efficiency experimental configuration for a self-referenced lattice comparator with a 'brush beam' of synchrotron radiation from a bending magnet and two linear position-sensitive photon-counting-type X-ray detectors. The efficiency is more than ten times greater compared with the 'pencil-beam' configuration and a pair of zero-dimensional detectors. A solution for correcting the systematic deviation of *d*-spacing measurements caused by the horizontal non-uniformity of the brush beam is provided. Also, the use of photon-counting-type one-dimensional detectors not only improves the spatial resolution of the measurements remarkably but can also adjust the sample's attitude angles easily.

1. Introduction

In 2003, Zhang *et al.* (2003) proposed a method to measure the *d*-spacing of silicon crystals using the wavelength selectivity of synchrotron radiation (SR) by using a self-reference lattice comparator (SRLC). The use of high-intensity SR solves the problem of *d*-spacing mapping measurements for large-scale samples, meaning that this method can be used to characterize the perfection of the ²⁸Si crystals used in the International Avogadro Coordination (IAC) project (Fujimoto *et al.*, 2011; Waseda *et al.*, 2015). The uniformity of the silicon crystal lattice spacing was evaluated by the SRLC with a resolution of 3×10^{-9} .

Although previous experiments using lattice comparators could characterize large-scale samples through point-by-point mapping measurements, this is not efficient. This method normally takes more than 20 h to measure a sample of size 20 mm × 40 mm. The poor signal-to-noise ratio (S/N) is not conducive to further reducing the spot size and improving the spatial resolution of the measurements when using the photon-current mode of a photodiode to detect the diffraction intensities. Therefore, a point-by-point mapping method is not suitable for measuring samples of large size or quantity. Furthermore, because of the long measurement time, instabilities of temperature and wavelength strongly influence the measurement precision. Also, a pair of specially designed detectors with spatial resolution is required for the previous SRLC, which makes the experiments demanding in adjusting the attitude angles (yaw angle and roll angle) of the sample.

At present, the main force of third-generation SR facilities is undulator radiation. However, with the technological developments of SR optics and detectors, the bending-magnet



beam can also play a wider role as it has advantages in terms of a continuous spectrum and a sector output beam whose merits are not found in undulator radiation. To cut the sector of a bending-magnet beam into a ‘pencil beam’ results in a significantly worse performance than when using undulator radiation. In addition, making full use of the large light spots distributed along the sector in combination with a one- or two-dimensional photon-counting detector greatly improves the scanning-measurement efficiency and also makes effective use of SR from the bending magnet. In this case, mapping measurements are more like painting with a ‘brush’ than plotting with a ‘pencil’. However, the use of a ‘brush beam’ instead of a ‘pencil beam’ introduces a series of uniformity problems that require raw-data correction procedures. Initial results have been published by Yang *et al.* (2019). The current article mainly discusses the effect of the beams’ horizontal angular divergence during comparative measurement when using a brush beam from an SR bending-magnet source, as well as that of the lattice inhomogeneity of a monolithic double channel-cut monochromator (MDCM) – the key component in the SRLC – on the measurement results, and the article further proposes a method to correct these problems. The current article also provides the brush-beam scanning measurement results of using the improved SRLC on the d -spacing of a monocrystalline ^{28}Si sample 9.R1 (Waseda *et al.*, 2015, 2017), which was used in the IAC project (Andreas *et al.*, 2011a,b).

2. The SRLC using a brush beam and one-dimensional photon-counting detectors

A schematic diagram of the SRLC when using a brush beam of SR from a bending magnet and a pair of one-dimensional (1D) photon-counting detectors is shown in Fig. 1. The bending-magnet SR beam is preliminary monochromated by an Si 111

double-crystal monochromator and further monochromated by an MDCM. The central direction of the brush beam incident to the MDCM and sample is parallel to the $[10\ 1\ 1]$ direction in the experimental configuration. The diffraction angle θ is rotated around the $[\bar{1}55]$ direction, and the yaw angles of the MDCM and the sample are rotated around the $[01\bar{1}]$ direction. The vertical beam divergence equals the acceptance angle of the MDCM, whereas the horizontal beam divergence depends on the horizontal slit on the beamline and the blade width of the MDCM. The MDCM consists of two channel cuts with two diffraction planes of $(10\ 0\ 2)$ and $(10\ 2\ 0)$, with an intrinsic energy resolution of 1.7×10^{-6} at 11.754 keV. The X-ray beam emitted from the MDCM is then projected onto the sample and reflected by the $(10\ 0\ 2)$ and $(10\ 2\ 0)$ diffraction planes of the sample crystal with normal direction $[100]$, and finally captured by the two 1D array detectors. When the temperature, attitude angles and other parameters of the sample are well adjusted, the relative difference of the d -spacing can be expressed by the following equation,

$$\frac{\Delta d}{d} = \frac{d_{\text{sample}} - d_{\text{MDCM}}}{d_{\text{MDCM}}} = \cos \theta_B \left(\frac{\gamma}{2} - \frac{\gamma_{\text{offset}}}{2} \right), \quad (1)$$

where

$$\frac{\gamma_{\text{offset}}}{2} = \frac{1}{26} \frac{\delta}{\sin 2\theta_B}, \quad (2)$$

and d_{sample} and d_{MDCM} are the respective d -spacing values of the sample and the MDCM. θ_B is the Bragg angle for 11.754 keV, and γ (~ 5 arcsec) is the angular interval between the two diffraction beams $(10\ 0\ 2)$ and $(10\ 2\ 0)$. γ_{offset} is the offset of the refractive effect caused by an asymmetry-factor inconsistency between the sample and the MDCM, and δ is the real part of the refraction index. This offset is ~ 0.1 arcsec. Therefore, measurement of the d -spacing corresponds to measurement of the γ value.

The two detectors used in the experiment are MYTHEN 1K detectors, which are photon-counting-type detectors with 1280 channels of $50\ \mu\text{m} \times 8000\ \mu\text{m}$ ($W \times L$) silicon-based strips sensors, which can avoid the problem of dark current and improve the S/N of the diffraction intensity. The detectors’ maximum counting rate of each channel is 10^6 counts s^{-1} . Therefore, the new detectors can collect the diffraction signal from a smaller area on the crystal than before and the brush beam is suitable for measuring a wider area on the sample simultaneously.

Position resolution is also very beneficial for the adjustment of the MDCM and sample attitudes within the SRLC, allowing for direct observation of the spots after the MDCM or

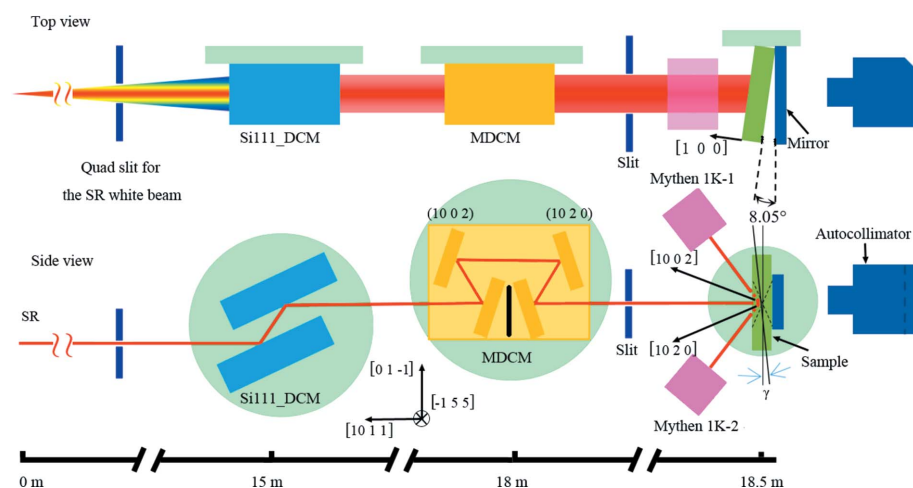


Figure 1 Top and side views of the experimental configuration. The brush beam from the SR bending magnet is preliminary monochromated by the double-crystal monochromator and further monochromated by the MDCM, and then projected onto the sample. The diffraction beams of the $(10\ 2\ 0)$ and $(10\ 0\ 2)$ planes in the sample are captured by two 1D photon-counting detectors.

the sample diffractions, which is helpful for adjusting the attitude angles of the sample.

3. Effects of using a brush beam in an experimental *d*-spacing measurement

In a pencil-beam scanning experiment, the X-ray wavelength is fixed and the only variable parameter is the location on the sample, which is a type of point-to-point measurement. Therefore, as long as the γ value at each point on the sample is measured, the *d*-spacing value at that point can be obtained through equation (1). When using a brush beam, because of its horizontal angular divergence, as well as the *d*-spacing homogeneity of the monocrystalline silicon constituting the MDCM, the brush beam passing through the MDCM also has a horizontal angular divergence and a wavelength distribution. Therefore, when performing line-scan measurements, even if the *d*-spacing of the sample to be measured is homogeneous, the difference in horizontal angular divergence and wavelength distribution of the brush beam will cause an apparent change in γ value on the brush footprint. This is a type of line-to-line measurement, which requires a correction of the systemic deviation due to widening of the X-ray beam from a pencil beam to a brush beam. In principle, for MDCMs using perfect monocrystalline silicon, the sine of the diffraction angle θ_φ of the incident MDCM can be expressed by

$$\sin \theta_\varphi = \sin \theta_0 \cos \varphi, \quad (3)$$

where θ_0 is the diffraction angle when the incidence of the pencil beam is perpendicular to the MDCM, and φ is the angle deviating from the central incident direction in a spot of the brush beam.

The wavelength of the output beam from the MDCM can be expressed by (Deutsch & Hart, 1982)

$$\lambda(\varphi) = 2d \cos \frac{\beta_0}{2} \cos \varphi, \quad (4)$$

where β_0 is the angle between the two diffraction planes of the MDCM.

Then, the differential of the diffraction angle $\Delta\theta$ and the differential of the relative wavelength $\Delta\lambda/\lambda$ are given by equations (5) and (6), respectively,

$$\Delta\theta = -\frac{1}{2} \tan \theta_B \varphi^2, \quad (5)$$

$$\frac{\Delta\lambda}{\lambda} = -\frac{1}{2} \varphi^2. \quad (6)$$

It should be noted that when the brush beam with the wavelength distribution expressed in equation (4) is incident on the sample according to the angle expressed in equation (3) (meaning

that the attitude of the sample is exactly the same as that of the MDCM), the change of the relative *d*-spacing measurement value caused by the beam factor is zero, which is expressed as

$$\frac{\Delta d}{d} = \frac{\Delta\lambda}{\lambda} - \frac{\Delta\theta}{\tan \theta_B} = 0. \quad (7)$$

However, the lattice of the MDCM used in practice is not perfectly homogeneous. It is also impossible to ensure that the attitude of the sample is exactly the same as that of the MDCM in the actual process. Lattice imperfections of the MDCM will cause the output beam wavelength distribution to deviate from the theoretical value described by equation (6), and the inconsistency between the attitude of the sample and that of the MDCM will cause the angle incident on the sample to deviate from the theoretical value described by equation (4). The deviation of the wavelength is unpredictable, while the deviation caused by the attitude angle is predictable. Therefore, correction of the system is still necessary. The following two paragraphs describe the system correction method that we used in the experiment. In this method, we use a sample to normalize each point in the brush beam directly, without distinguishing the causes of the measurement deviation.

Fig. 2 reflects the changes from pencil beam to brush beam in the SRLC. The previous SRLC used a pencil beam and a pair of point detectors to make a point-by-point scan on the sample. The improved SRLC uses a brush beam and two linear detectors. Because of the different parameters in the horizontal direction of the brush beam, the observations must

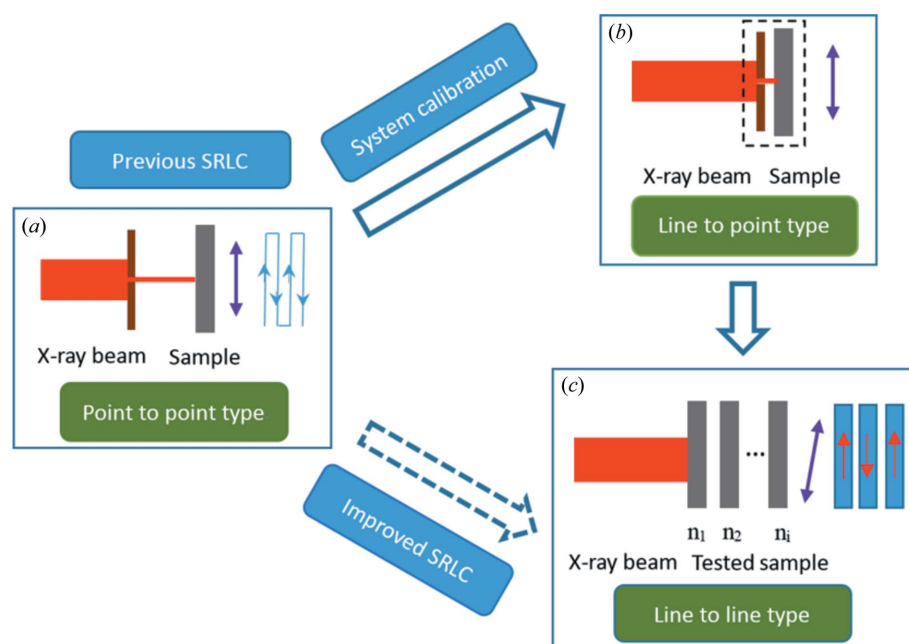


Figure 2 Schematic diagram of the SRLC improvement from the pencil beam to the brush beam. (a) SRLC using the pencil-beam scan in point-to-point mode. (b) The system-calibration process of the SRLC when using the brush beam; the correction-factor set is obtained in a line-to-point manner. (c) The brush-beam scan process of the SRLC. The purple arrow (two-way arrow) in the figure represents the moving direction of the sample-stages table during the measurement. The stages in (a) and (b) move parallel to the paper direction ([155] direction), and the stages in (c) move perpendicular to the paper direction ([011] direction). The blue arrow in (a) indicates the point-by-point mapping mode of the pencil beam, while the blue rectangle in (c) indicates the area where the mapping mode is like painting by a brush.

be corrected to obtain the unbiased d -spacing distribution of the sample being measured systematically. This systematic correction may be achieved by using a point-to-line correction to determine the correction factors for each position of the brush beam. Using this set of renormalization factors to correct the measurements of the sample in the line-to-line measurement mode, the brush-beam scanning measurement can be achieved.

We use the following method to obtain a system correction-factor set. A narrow slit is placed in front of the sample and can be moved horizontally along with the sample. A scan through the slit is used to obtain diffraction results throughout all positions of the brush beam [Fig. 2(b)]. This operation is to measure the same d -spacing using fine X-rays at different points along the brush beam. By normalizing the observations at each point, the brush-beam correction-factor set for line-scan measurement data is obtained. When the measured values of the brush beam are corrected by the systematical correction-factor set, the measurements of the sample d -spacing distribution can be achieved quickly and efficiently.

4. Adjustment of experimental configuration

Based on the above description, an experiment was performed at beamline BL3C of the Photon Factory of the High Energy Accelerator Research Organization (KEK, Tsukuba, Japan), configured as in Fig. 1. The quad slit on the beamline fixes the size of the incident beam inside the experimental station to 20 mm × 1 mm (H × V). The MDCM is installed on a KOUZH KTG-15 goniometer with a resolution of 0.005 arcsec, 18 m downstream of the SR source, and is placed inside a temperature-controlled aluminium cast box. The short-time temperature stability of the box can attain to 0.001°C. The sample is set inside the box ~0.5 m downstream of the MDCM. The box is also equipped with two stages to adjust the attitude angles of the sample. The sample is placed on the rolling stage, and the rolling stage is mounted on the yawing stage. The diffraction angle is controlled by a piezo-ceramic-driven flexible hinge stage, and the diffraction interval is measured by an autocollimator and a flat mirror mounted on the rear of the sample box. Two MYTHEN 1K detectors are placed in front of the sample box with a Mylar film window to capture the diffracted beams from the (10 0 2) and (10 2 0) lattice planes.

The first step in the experiment is to adjust the Si 111 double-crystal monochromator to be in the optimal position, matching with the MDCM. That is, the central wavelength of the outgoing beam from the Si 111 double-crystal monochromator is precisely adjusted to the wavelength that can pass through the MDCM. Then, the attitude of the MDCM is adjusted via help from the sample diffractions, so that the [155] direction can be adjusted to perpendicular to the incident beam. After the Si 111 double-crystal monochromator and the MDCM are adjusted to their appropriate positions, the MDCM is rotated and the position-resolution rocking curve for the rotating MDCM is obtained by the MYTHEN 1K (Fig. 3). The MDCM is placed on the maximum spot of the

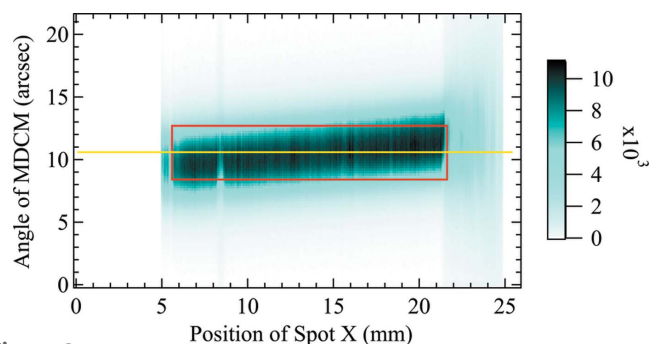


Figure 3 Spots are visible on the MYTHEN 1K when rocking the MDCM. The position indicated by the yellow line is the set position of the MDCM. In this case the red rectangular frame represents a spot of 16 mm × 0.3 mm ($X \times Z$); it is the available throughput beam spot of the MDCM.

throughput beam (the position shown by the yellow line in Fig. 3), behind which the spot size available has dimensions of 16 mm × 0.3 mm (the red rectangular frame area in Fig. 3). The central energy is 11.754 keV and the Bragg angle θ_B is 82.03°.

The sample's attitude angle is adjusted as follows. It is more convenient than the previous method to use a linear detector to adjust the sample's attitude angles because the changes of the diffraction-spot position can be detected directly by a position-sensitive detector. When adjusting the yaw angle of the sample, the upper and lower diffraction spots move in the same direction; when adjusting the roll angle of the sample, the upper and lower diffraction spots move in the reverse direction (Fig. 4). This process was greatly simplified by the 1D detectors.

After the positioning of the Si 111 double-crystal monochromator, the positions and attitude angles of the MDCM and those of the sample are well adjusted; the experimental configuration of the system calibration according to Fig. 2(b) is shown in Fig. 5. A slit of width 0.5 mm is set in front of the sample. Then the slit and the sample are moved together

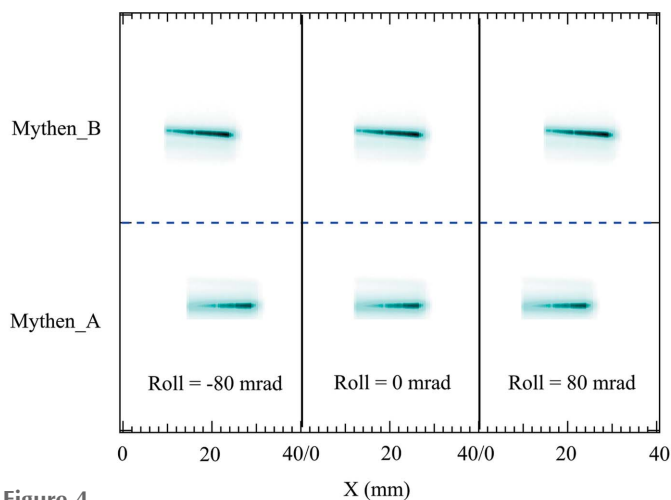
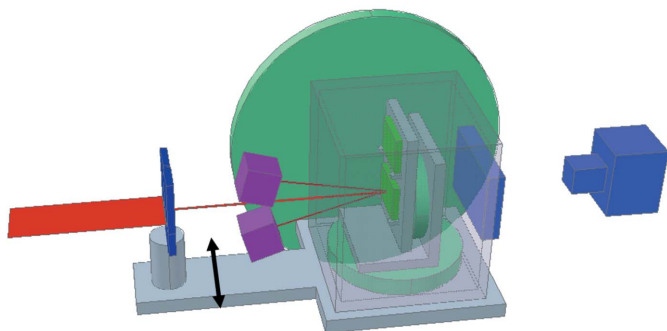


Figure 4 The respective positions of the diffracted spots of the (10 0 2) and (10 2 0) diffraction planes of the sample on the two MYTHEN 1K detectors when the roll angle is adjusted. When the two spots appear in the same lateral position, the appropriate roll angle has been reached.

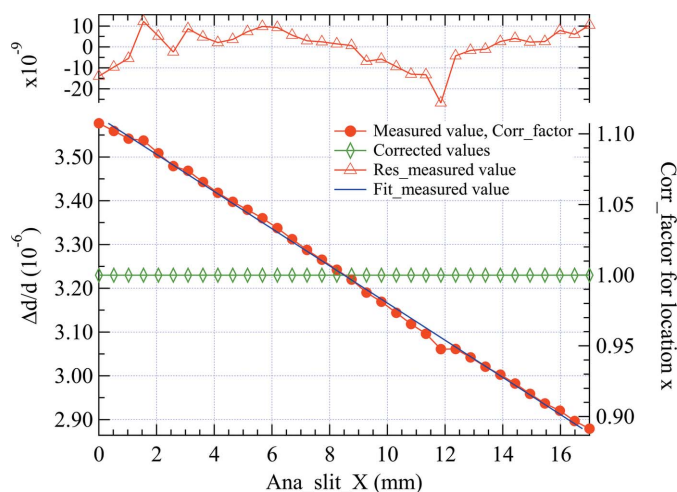

Figure 5

Schematic diagram of the calibration process for the angle divergence of the brush beam and the lattice inhomogeneity of the MDCM. A slit of width 0.5 mm installed in front of the sample is used for scanning horizontally along the beam. The sample is rotated at each position and the d -spacing is measured at the same point on the sample by using the beam at different horizontal positions of the brush beam. Finally, based on this measurement, the measurement results of the brush beam are corrected.

across the beam along the horizontal direction, obtaining the γ values measured for the same d -spacing of the sample by the pencil beam at different horizontal positions, and the raw $\Delta d/d$ is obtained. After normalizing the measured values, the system correction-factor set of the SRLC using a brush beam is obtained. Once the above process is completed, $\Delta d/d$ of the sample can be measured directly by the brush beam.

5. Data processing and discussion

The red circles (left axis) in Fig. 6 show the relative measurements for the same d -spacing for each pencil beam generated by a slit from the brush beam. The maximum deviation of $\Delta d/d$ is $\sim 7 \times 10^{-7}$ and is basically linear with the analyser slit position (φ angle). The blue line in Fig. 6 is fitting by linear equation. The red triangles in Fig. 6 are the residual


Figure 6

Systematic correction results. Red circles (left axis) are the relative measurements of the same d -spacing for different horizontal positions of the brush beam, and the right axis is the system correction-factor scale. After the systematic correction, the red circles become the green squares, which give a uniform distribution through the brush beam.

between the measured value and the linear fitting result. The slope of the blue line is $\sim -4 \times 10^{-8}$. The slope becomes -7.8×10^{-7} when the horizontal axis is φ . Using equations (5)–(7), when there is a deviation between the yaw angle of the sample and the MDCM, $\Delta d/d$ can be expressed as

$$\frac{\Delta d}{d} = \frac{\Delta \lambda}{\lambda} - \frac{\Delta \theta}{\tan \theta_b} = -\frac{1}{2} \varphi^2 + \frac{1}{2} (\varphi + \Delta \varphi)^2.$$

Then,

$$\frac{\Delta d}{d} = \Delta \varphi \varphi + \frac{1}{2} \Delta \varphi^2. \quad (8)$$

Therefore, it can be estimated that there is a deviation of 0.78 mrad between the yaw angle of the sample and the MDCM. The residuals of the $\Delta d/d$ linear fitting are caused by other factors, such as (i) lattice imperfection or stress distribution from the crystal used in the production of the MDCM, (ii) imperfection or stress in the lattice of the upstream Si 111 double-crystal monochromator, (iii) deviation of the roll angle between sample and MDCM, (iv) temperature stability, *etc.* According to the description of the system-deviation correction method in Section 3, the measured result of $\Delta d/d$ can be renormalized directly without considering these specific factors. The green squares in Fig. 6 show the results after renormalization correction. The red circles (right axis) in Fig. 6 show the system correction factors, which are obtained by dividing the measured values by the corrected values.

Fig. 7 shows the measurements on a monocrystalline silicon sample 9.R1 using the improved SRLC, where the spatial resolution is 0.5 mm \times 0.5 mm. Figs. 7(a) and 7(b) show the raw data and corrected results before and after, respectively, with the brush-beam systematic correction-factor set. The results shown in Fig. 7(b) are essentially consistent with the previous point-by-point scan results (Waseda *et al.*, 2017). Benefiting from the photon-counting mode of the 1D detector, with a better S/N than the photodiode, the diffraction area can be reduced under the same incident-beam intensity, increasing its spatial resolution by 0.5 mm \times 0.5 mm from the previous 1 mm \times 1 mm.

The horizontal width of the MDCM used in the experiment is 20 mm, but when the horizontal width of the incident beam into the MDCM is 20 mm it is found that the maximum horizontal width of the output light spot can only reach 16 mm. In fact, the effect of horizontal divergence of the brush beam is equivalent to that of the adjustment of the MDCM's tilt angle. However, it is found that when adjusting the tilt angle of the MDCM the entire spot of width 20 mm can be observed behind the MDCM. In addition, the spot shape behind the MDCM shown in Fig. 3 is inclined. We began to suspect that this might be due to the roll angle of the MDCM or the upstream Si 111 double-crystal monochromator being inappropriate. However, the inclined state in the image cannot be improved when we adjust the roll angle. In addition, when we use another index of the MDCM, *i.e.* 771 instead of 10 2 0, we find that the same image presents a horizontal state. So, it is confirmed that defects or stresses exist in some parts of the MDCM. The main factor limiting further increase in

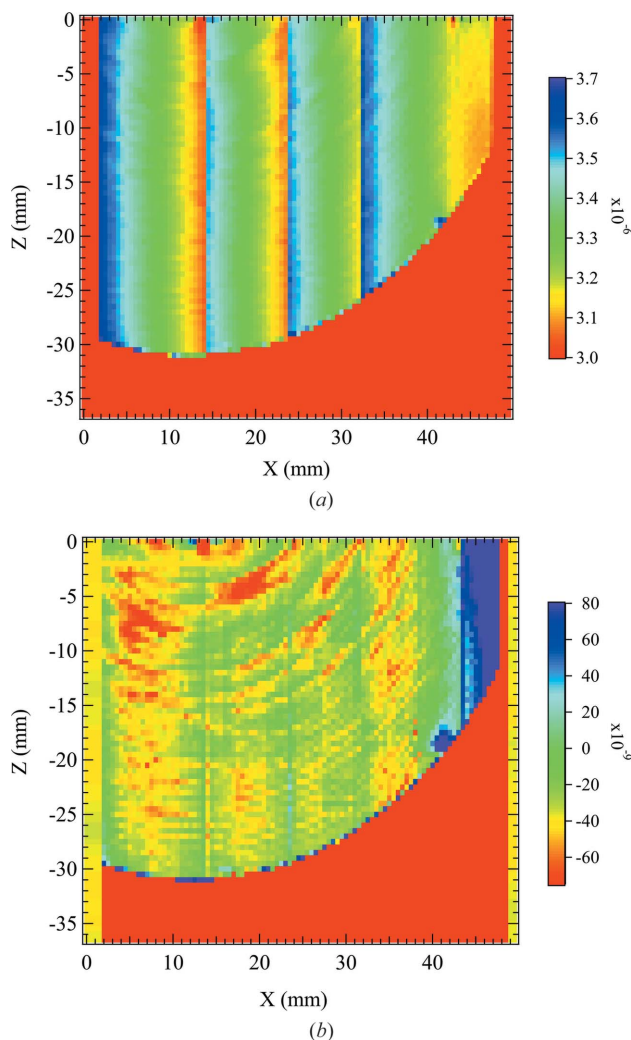


Figure 7
Measurements on a monocrystalline silicon sample 9R1 using the improved SRLC, where the spatial resolution is $0.5\text{ mm} \times 0.5\text{ mm}$. (a) Raw data from the measurement by the brush-beam mapping. (b) The result after correction.

measurement efficiency is the width of the beam behind the MDCM. In addition, the maximum spatial resolution of the MYTHEN 1K detector is $50\text{ }\mu\text{m}$. However, when using a single channel of $50\text{ }\mu\text{m}$, the maximum single-pixel counting rate is only $\sim 500\text{ counts s}^{-1}$, showing insufficient signal strength. Therefore, in the experiment, ten channels are combined into one group to solve this problem. To obtain higher spatial resolution, a higher light intensity and smaller slit for correction should be adopted.

6. Conclusions

Although the intensity of the beam from a bending magnet is lower than from an insertion device, it has the characteristics of a continuous spectrum and large spot size. If the advantage of the large spot of the bending-magnet beam can be utilized completely, in combination with the advanced 1D/2D X-ray detector, the overall efficiency will not be lower than that of the point-by-point scanning mode using a strong beam. In this

article, the influence of the brush beam on the measurement of d -spacing has been dealt with theoretically and a convenient high-efficiency accurate correction method has been provided through experimentation. This makes it possible for the SRLC to efficiently characterize large sample d -spacing using a brush SR beam. As a result, the previous SRLC is improved using a brush beam of SR and a pair of 1D X-ray photon-counting detectors instead of the original pencil beam and zero-dimensional photodiode detector. By correcting the systematic deviation caused by the divergence of different horizontal position angles of the brush beam for the same d -spacing, the point-to-point scanning measurement is replaced by line-to-line brushing, which shows that the efficiency of measurement has been improved by more than ten times. The experimental time has been shortened from the original from more than 20 h to less than 2 h. This method not only improves the utilization efficiency of the SR bending-magnet source but also makes full use of the technical characteristics of the MYTHEN 1K detector to obtain higher spatial resolution. Also, the high spatial resolution and high S/N measurement results have further verified the performance of the photon-counting detector which is better than that of the current signal-mode detector. Because the measurement process of the improved SRLC has only made corrective changes from the pencil beam to the brush beam and the correction process is still achieved by the point-to-point measurement, the precision of the measurement results can be maintained to be the same as before. Measurements of the monocrystalline silicon sample 9R.1 demonstrate the reliability of the improved SRLC. Therefore, the improved SRLC, with MYTHEN 1K detectors and the brush beam, will be more competent for the characterization of large-scale silicon crystals.

Funding information

The experiment was carried out under PAC of 2016S2-002 of the Photon Factory. At the same time, we would like to thank the Innovation Fund of the Institute of High Energy Physics, Chinese Academy of Sciences for its support.

References

Andreas, B., Azuma, Y. & Bartl, G. (2011a). *Metrologia*, **48**, S1–S13.
 Andreas, B., Azuma, Y., Bartl, G., Becker, P., Bettin, H., Borys, M., Busch, I., Gray, M., Fuchs, P., Fujii, K., Fujimoto, H., Kessler, E., Krumrey, M., Kuetgens, U., Kuramoto, N., Mana, G., Manson, P., Massa, E., Mizushima, S., Nicolaus, A., Picard, A., Pramann, A., Rienitz, O., Schiel, D., Valkiers, S. & Waseda, A. (2011b). *Phys. Rev. Lett.* **106**, 030801.
 Deutsch, M. & Hart, M. (1982). *Phys. Rev. B*, **26**, 5558–5567.
 Fujimoto, H., Waseda, A. & Zhang, X. W. (2011). *Metrologia*, **48**, S55–S61.
 Waseda, A., Fujimoto, H., Zhang, X. W., Kuramoto, N. & Fujii, K. (2015). *IEEE Trans. Instrum. Meas.* **64**, 1692–1695.
 Waseda, A., Fujimoto, H., Zhang, X. W., Kuramoto, N. & Fujii, K. (2017). *IEEE Trans. Instrum. Meas.* **66**, 1304–1308.
 Yang, J. L., Hu, L., Zhu, Y., Diao, Q., Hong, Z., Zhang, X., Waseda, A. & Fujimoto, H. (2019). *AIP Conf. Proc.* **2054**, 060016.
 Zhang, X., Sugiyama, H., Ando, M., Imai, Y. & Yoda, Y. (2003). *J. Appl. Cryst.* **36**, 188–192.